JACS
JOURNAL OF THE AMERICAN CHEMICAL SOCIETY
Article
pubs.acs.org/JACS

Formation Pathway for LTA Zeolite Crystals Synthesized via a Charge Density Mismatch Approach

Min Bum Park,[†] Yoorim Lee,[†] Anmin Zheng,[‡] Feng-Shou Xiao,[§] Christopher P. Nicholas,[∥] Gregory J. Lewis,[∥] and Suk Bong Hong*[,†]

[†]Department of Chemical Engineering and School of Environmental Science and Engineering, POSTECH, Pohang 790-784, Korea
[‡]State Key Laboratory of Magnetic Resonance and Atomic and Molecular Physics, Wuhan Institute of Physics and Mathematics, Chinese Academy of Sciences, Wuhan 430071, P. R. China
[§]Department of Chemistry, Zhejiang University, Hangzhou 310028, P. R. China
[∥]UOP LLC, Des Plaines, Illinois 60017, United States

Supporting Information

ABSTRACT: A solid understanding of the molecular-level mechanisms responsible for zeolite crystallization remains one of the most challenging issues in modern zeolite science. Here we investigated the formation pathway for high-silica LTA zeolite crystals in the simultaneous presence of tetraethylammonium (TEA^+), tetramethylammonium (TMA^+), and Na^+ ions as structure-directing agents (SDAs) with the goal of better understanding the charge density mismatch synthesis approach, which was designed to foster cooperation between two or more different SDAs. Nucleation was found to begin with the formation of *lta*-cages rather than the notably smaller *sod* and *d4r*-cages, with concomitant incorporation of TMA^+ and Na^+ into a very small amount of the solid phase with a low Si/Al ratio (ca. 2.5). The overall characterization results of our work demonstrate that *sod*-cages are first built around the preorganized *lta*-cages and that *d4r*-cages are in turn constructed by the progressive addition of low-molecular-weight (alumino)silicate species, which promotes the formation and growth of embryonic LTA zeolite crystals. We also show that the crystal growth may take place by a similar process in which TEA^+ is also incorporated, forming a single LTA zeolite phase with a higher Si/Al ratio (ca. 3.3).

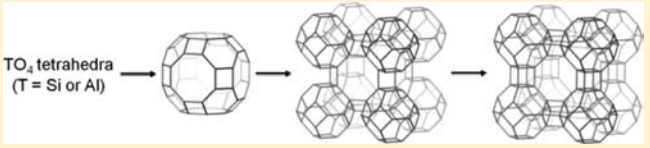

INTRODUCTION

Despite the great success that zeolites, with channels and cavities of molecular dimensions, have had as industrial adsorbents, ion exchangers, and catalysts,[1] understanding how they nucleate and grow remains one of the most challenging issues in modern zeolite science. These highly porous crystals are metastable in nature,[2] so their wide structural diversity must rely on the nucleation process, which determines the phase selectivity of the crystallization. According to the secondary building unit (SBU) theory proposed by Barrer,[3] zeolites can grow from the structural elements of their final framework. To date, a wide variety of silicate oligomers, including cagelike double-ring species (*d3r*, *d4r*, *d5r*, and *d6r*), have been identified in aqueous alkaline and/or tetraalkylammonium silicate solutions by ^{29}Si NMR spectroscopy.[4] Apart from the intense controversy concerning the SBU concept itself, however, the existence of zeolite building units with greater than 12 tetrahedral atoms (T-atoms) in the solution or solid phase has not been experimentally evidenced to date. Furthermore, no attempts to elucidate unequivocally the pathways for forming even the simplest zeolites from their SBUs (if they really exist) have yet been successful.

Zeolite A (LTA) with a framework Si/Al ratio of ca. 1, which is one of the most widely used model systems for studies of zeolite crystallization mechanisms, has been repeatedly proposed to crystallize by self-assembly of *d4r*-cages even in the presence of organic structure-directing agents (SDAs).[5] As shown in Figure 1, the LTA structure can be built from 14-hedral ($[4^6 6^8]$) *sod*-cages with 24 T-atoms that are linked through *d4r* units, producing a 26-hedral ($[4^{12}6^8 8^6]$) *lta*-cage with 48 T-atoms in the center of its unit cell.[6] UZM-9, a silica-rich LTA zeolite, is among the zeolites that have been synthesized using the charge density mismatch (CDM) approach developed by researchers at UOP.[7] This zeolite has

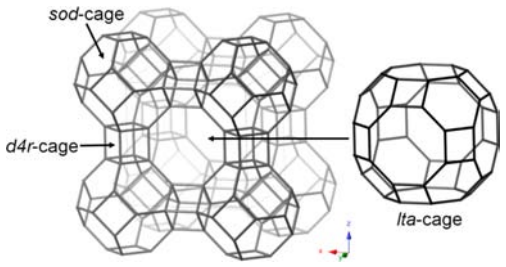

Figure 1. LTA structure and its three different composite building units.

Received: October 5, 2012
Published: November 27, 2012

dx.doi.org/10.1021/ja309831e | J. Am. Chem. Soc. 2013, 135, 2248−2255

been reported to crystallize using both tetramethylammonium (TMA^+) and tetraethylammonium (TEA^+) ions, the two most common organic SDAs, together with Na^+.[7a]

The CDM approach to zeolite synthesis was initially proposed as a cheaper alternative to the trend of using ever more complicated quaternary ammonium species designed to be a "hand-in-glove" fit between the SDA and the zeolite pore structure.[1a] One serious problem that needs to be addressed in a multiple-SDA system is how to prevent the SDAs from directing the synthesis of multiple structures, that is, how to achieve cooperation between multiple SDAs. To gain control over the crystallization process, we first constructed a synthesis system that cannot condense or crystallize. This CDM synthesis mixture consists of an aluminosilicate solution that has a relatively low Si/Al ratio and thus has the potential to make a zeolite framework with a high negative charge. The solution also contains a large, low-charge-density SDA such as TEA^+, which cannot efficiently balance the relatively high aluminosilicate negative charge in a manner that provides extensive condensation or crystallization,[7] even after heating at typical synthesis temperatures.

Therefore, the CDM aluminosilicate solution contains a barrier to crystallization that can also depend on the hydroxide level. Typically, higher hydroxide levels shift the aluminosilicate speciation to smaller and more highly charged species, increasing the difficulty with which condensation occurs. This implies that one must break down such a crystallization barrier to effect crystallization of a zeolite. The CDM aluminosilicate solution is perturbed with small amounts of high charge density SDAs (e.g., Na^+ and TMA^+), which are highly effective at breaking down this barrier and inducing condensation or crystallization. Cooperation of multiple SDAs results because these SDAs need one another to complete the crystallization. By itself, TEA^+ is an ineffective SDA in this system and requires assistance from Na^+ and TMA^+ ions to effect crystallization. To that end, the latter two smaller SDAs are kept at levels low enough that they cannot dominate or complete the crystallization and need assistance from TEA^+. Hence, TEAOH serves as the hydroxide source for zeolite synthesis and is present in large excess relative to TMA^+ and Na^+ ions. A consequence of the CDM approach is that over the course of the crystallization, the aluminosilicate species are largely present in solution.

Clearly, the situation described above is far from traditional alkali-rich zeolite syntheses in which the aluminosilicate species are sparingly soluble and most of the synthesis mixture initially resides in an amorphous aluminosilicate gel. Delicately attacking the barrier to crystallization with low amounts of Na^+ and TMA^+ at low temperatures slows the course of the synthesis, enhancing the ability to characterize the fundamental steps in LTA zeolite syntheses. Here we present indirect but secure experimental evidence that the CDM synthesis of high-silica LTA zeolite in the $TEA^+/TMA^+/Na^+$ mixed-SDA system involves the initial formation of *lta*-cages as nucleation centers, which is contrary to the proposed mechanism for traditional LTA zeolite syntheses.[5d] With the combined aid of experimental and theoretical approaches, we also show that the construction of *sod*-cages around the preorganized *lta*-cages is followed by the construction of *d4r*-cages. Finally, the nature of the roles of the SDAs in this LTA crystallization is described.

EXPERIMENTAL SECTION

Synthesis. A clear synthesis solution with the composition $8.0TEAOH/0.5TMACl/0.5NaCl/1.0Al[O(s\text{-}Bu)]_3/8.0TEOS/240H_2O$ was prepared by combining tetramethylammonium chloride (TMACl, 97%, Aldrich), tetraethylammonium hydroxide (TEAOH, 35% aqueous solution, Sachem), NaCl (≥99.5%, Aldrich), aluminum tri-*sec*-butoxide ($Al[O(s\text{-}Bu)]_3$, 97%, Aldrich), tetraethyl orthosilicate (TEOS, 98%, Aldrich), and deionized water. In a typical synthesis of high-silica LTA zeolite, $Al[O(s\text{-}Bu)]_3$ was mixed with a solution of TEAOH in water and stirred at room temperature for 2 h. To this clear solution, a given amount of TEOS was added. After being aged at 95 °C for 1 day, the resulting solution was mixed with a solution of TMACl and NaCl in water and stirred at room temperature for 1 day. The final synthesis solution was filtered with 200 nm Whatman filter papers and characterized by multinuclear solution NMR spectroscopy or subjected to crystallization within Teflon-lined 23 mL autoclaves under rotation (60 rpm) at 100 °C for a total period of 18 days. Prior to NMR characterization or crystallization, no special care was taken to eliminate all of the 2-butanol and ethanol molecules in the synthesis solution generated by hydrolysis of the Al and Si sources, respectively. The solid products and mother liquors were separated by centrifugation (15 000 rpm, 10 min). The recovered solids were redispersed in deionized water using an ultrasonic bath (100 W, 42 kHz) for 60 min with subsequent centrifugation, which was repeated three times. Finally, the resulting solids were dried overnight at room temperature. If required, some solid products obtained in this study were refluxed twice in 1.0 M $NaNO_3$ solutions (1 g of solid/100 mL of solution) for 4 h.

ZK-4 (LTA) was synthesized from a starting aluminosilicate gel with the composition $3.0TMAOH/0.5NaCl/1.0Al(OH)_3/2.1SiO_2/55H_2O$. The reagents used included tetramethylammonium hydroxide (TMAOH, 25% aqueous solution, Aldrich), NaCl (≥99.5%, Aldrich), $Al(OH)_3{\cdot}H_2O$ (Aldrich), and colloidal silica (Ludox AS-40, DuPont). The final gel was stirred at room temperature for 1 day, charged into Teflon-lined autoclaves, and heated under rotation (60 rpm) at 80 °C for different times of up to 24 h. In addition, for comparison of the ^{13}C magic-angle-spinning (MAS) NMR chemical shift for TMA^+, a sodalite (SOD) sample with Si/Al = 3.4 was prepared by heating a clear solution with the composition $5.6TMAOH/0.75LiCl/1.0Al(OH)_3/2.0SiO_2/232H_2O$ under rotation (60 rpm) at 160 °C for 4 days.

Analytical Methods. Powder X-ray diffraction (XRD) patterns were recorded on a PANalytical X'Pert diffractometer (Cu Kα radiation) with an X'Celerator detector. The relative crystallinities of a series of solid products recovered at different time intervals were determined by comparing the areas of the intense X-ray peak around 2θ = 24.2°, corresponding to the (622) reflection of the LTA structure, with that of a fully crystallized sample. The yield of each product was calculated by dividing the mass of the product obtained after crystallization for a given time by the total mass of the oxide forms of all of the components in the synthesis mixture except water. IR spectra in the structural region were recorded on an ABB Bomen MB 104 FT-IR spectrometer using the KBr pellet technique. The concentration of solid sample in the KBr pellets was kept constant at 0.02 g of sample/g of KBr, and 256 scans were accumulated to obtain the IR spectra. Thermogravimetric analysis (TGA) was performed on an SII EXSTAR 6000 thermal analyzer, and the weight losses related to the combustion of organic SDAs were further confirmed by differential thermal analysis (DTA) using the same analyzer. Elemental analyses for Si, Al, and Na were carried out using a Jarrell-Ash Polyscan 61E inductively coupled plasma spectrometer in combination with a PerkinElmer 5000 atomic absorption spectrophotometer. The C, H, and N contents of the samples were analyzed by using a Vario EL III elemental organic analyzer.

^{27}Al, ^{29}Si, and ^{13}C solution NMR measurements were carried out in 5 mm quartz tubes using a Bruker DRX-500 spectrometer. The ^{27}Al NMR spectra were recorded at a ^{27}Al frequency of 130.32 MHz with a $\pi/6$ rad pulse length of 3.0 μs, a recycle delay of 1 s, and acquisition of ca. 1000 pulse transients. The ^{29}Si NMR spectra were obtained at a ^{29}Si frequency of 99.35 MHz with a $\pi/6$ rad pulse length of 3.0 μs, a

dx.doi.org/10.1021/ja309831e | J. Am. Chem. Soc. 2013, 135, 2248−2255

recycle delay of 1 s, and acquisition of ca. 5000 pulse transients. The ^{13}C NMR spectra were recorded at a ^{13}C frequency of 125.77 MHz with a $\pi/6$ rad pulse length of 3.0 μs, a recycle delay of 2 s, and acquisition of ca. 1000 pulse transients. ^{27}Al, ^{29}Si, and ^{13}C MAS NMR measurements were performed on a Varian Inova 300 spectrometer at a spinning rate of 6.0 kHz. The ^{27}Al MAS NMR spectra were measured at a ^{27}Al frequency of 78.16 MHz with a $\pi/8$ rad pulse length of 1.8 μs, a recycle delay of 0.5 s, and acquisition of ca. 5000 pulse transients. The ^{29}Si MAS NMR spectra were measured at a ^{29}Si frequency of 59.59 MHz with a $\pi/2$ rad pulse length of 5.0 μs, a recycle delay of 30 s, and acquisition of ca. 3000 pulse transients. The ^{13}C MAS NMR spectra were recorded at a ^{13}C frequency of 75.43 MHz with a $\pi/2$ rad pulse length of 7.0 μs, a recycle delay of 2 s, and acquisition of ca. 10 000 pulse transients. The ^{27}Al chemical shifts are reported relative to $Al(H_2O)_6^{3+}$, and the ^{29}Si and ^{13}C chemical shifts are referenced relative to tetramethylsilane (TMS). Decomposition and simulation of the ^{29}Si and ^{13}C MAS NMR spectra obtained were carried out using the PeakFit curve-fitting program. One strong ^{13}C NMR line at 58.2 ppm, which must be due to the CH_3 ^{13}C NMR line of the occluded TMA^+ ions, was observed in the ^{13}C MAS NMR spectrum of as-made sodalite with Si/Al = 3.4.

Quantum-Chemical Calculations. Four different cage systems of the LTA structure, namely, a discrete *sod*-cage, a discrete *lta*-cage, and systems containing either 1 *lta*-cage + 12 *d4r*-cages or 1 *lta*-cage + 8 *sod*-cages + 12 *d4r*-cages, were employed to calculate the stabilization energies for various combinations of Na^+, TMA^+, and/or TEA^+ ions. The unit cell parameters and atomic coordinates for the LTA structure with space group $Fm\bar{3}c$ were taken from the original reference in the International Zeolite Association tabulation.[6] In the calculations, the terminal Si−H was fixed at a bond distance of 1.47 Å and oriented along the direction of the corresponding Si−O bond. Because of the hydrothermal nature of zeolite synthesis, the Na^+ ion in each cage system was assumed to exist as an octahedral $[Na(H_2O)_6]^+$ complex in which the Na−O bond distance was fixed at 2.37 Å, as in aqueous solution.[8] The combined theoretical model, an M06-2x/6-31+G-(d):MNDO ONIOM method,[9] was used to predict the geometries of various structures containing different combinations of SDAs. The M06-2X functional implicitly accounts for medium-range electron correlation and can describe dispersion interactions well in comparison with traditional DFT methods. Hence, it usually has the best performance for the non-covalent interactions.[10] The 5T cluster active center $[Al(SiO)_4]$ and adsorbed cations in the high-level layer were relaxed to preserve the integrity of the zeolite structure during the structure optimizations, while the rest of atoms were fixed at their crystallographic locations. The stabilization energy was calculated as the difference between the total energy of the absorption complex and the sum of the energies of the separated guest cations and the cluster model. All of the calculations were performed using the Gaussian 09 package.[11]

RESULTS AND DISCUSSION

Figure 2a shows the ^{29}Si NMR spectrum of a clear aluminosilicate synthesis solution with the composition 8.0TEAOH/0.5TMACl/0.5NaCl/1.0Al[O(*s*-Bu)]$_3$/8.0TEOS/240H_2O used in our work. This spectrum presents four major lines at −72.2, −80.8, −82.4, and −89.5 ppm due to the silicate monomer, dimer, cyclic trimer (*s3r*), and prismatic hexamer (*d3r*), respectively.[12] Also, there is at least one line at low-field relative to each of the latter three lines, assignable to the other small silicate or aluminosilicate species such as those described elsewhere.[12b] It is worth noting that the ^{29}Si line at −98.4 ppm attributed to the silicate cubic octamer (i.e., *d4r*), which has repeatedly been proposed to serve as a key building unit in the crystallization of zeolite A,[5d,e] is much weaker in intensity than the silicate *d3r* line. On the other hand, when the synthesis solution was heated under rotation (60 rpm) at 100 °C, the crystalline order detectable by powder XRD (in the range of a few unit cells[13]) was present after 18 h, and crystallization was complete after 6 days (Figure 3). Since the LTA material fully crystallized here has a somewhat lower Si/Al ratio (3.3) than the typical ratios (3.5−6.0) of UZM-9, it is designated as UZM-9LS, a low-silica (LS) version of UZM-9.

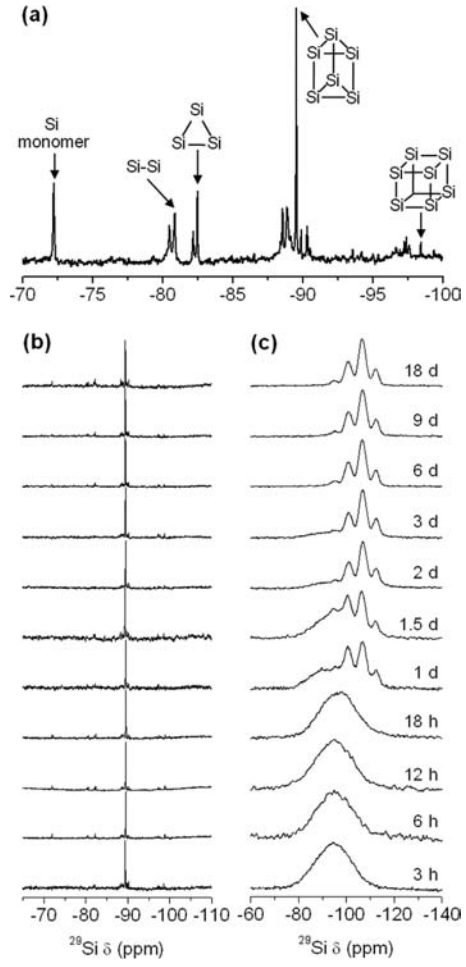

Figure 2. (a) ^{29}Si NMR spectrum of a starting synthesis solution with the composition 8.0TEAOH/0.5TMACl/0.5NaCl/1.0Al[O(*s*-Bu)$_3$]/8.0TEOS/240H_2O. (b) ^{29}Si NMR spectra of a series of mother liquors separated after UZM-9LS crystallization at 100 °C for different times. (c) ^{29}Si MAS NMR spectra of the solid products recovered after different periods of crystallization.

To follow the formation pathway for UZM-9LS, the mother liquors and solid products were recovered by centrifugation at different time intervals during the synthesis of this LTA-type zeolite at 100 °C and subjected to multinuclear solution and solid-state NMR measurements, respectively. The ^{29}Si solution NMR spectra in Figure 2b reveal that the concentration of silicate *d3r*-cages in all of the mother liquors was much higher than that of any of the other (alumino)silicate species, including *d4r* clusters. In fact, one previous molecular dynamics study[14] reported that the *d3r* cluster in aqueous solution can easily be stabilized by the presence of TEA^+ in addition to TMA^+, as in our synthesis solution. It is noteworthy that after only 3 h of heating, the relative intensities of the ^{29}Si lines other than the silicate *d3r* line became significantly weaker than those of the corresponding lines from the starting synthesis solution. Because this trend remained almost unchanged during the course of crystallization at 100 °C for 18 days, it is clear that a high concentration of *d4r*-cages was not necessarily present in

dx.doi.org/10.1021/ja309831e | J. Am. Chem. Soc. 2013, 135, 2248−2255

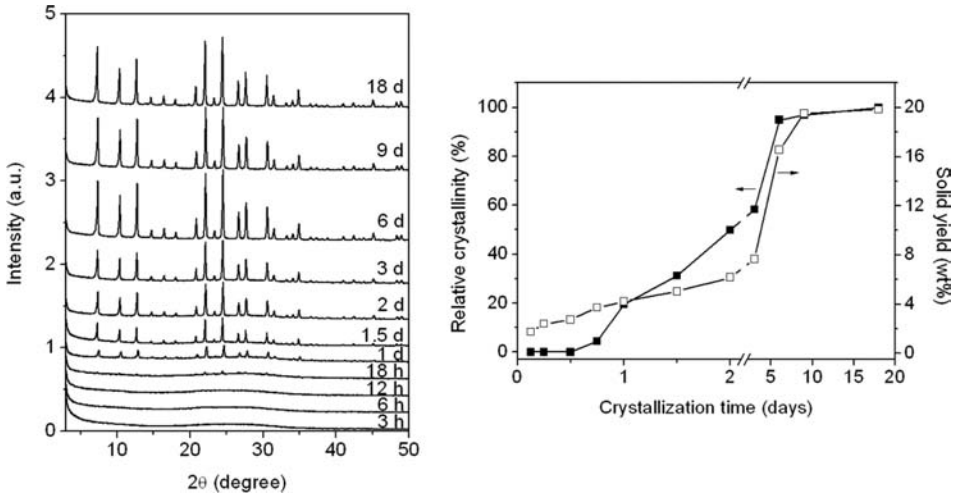

Figure 3. (left) Powder XRD patterns and (right) relative crystallinities and solid yields for a series of solid products obtained after crystallization at 100 °C for different times.

the liquid phase to facilitate the crystallization of UZM-9LS, in contrast to what has been proposed to date for zeolite A formation.[5d]

The ^{27}Al NMR spectrum of the starting synthesis solution (Figure S1 in the Supporting Information) shows signs of four components around 75, 70, 65, and 60 ppm, corresponding to $q^n(n\text{Si})$ species with n = 1−4, respectively.[15] However, the spectra of the mother liquors became featureless with increasing crystallization time, giving a broad line around 60 ppm after 6 days of heating. This suggests that the Al species in the solution phase during UZM-9LS synthesis were essentially nonmonomeric. We also found that the three "X-ray amorphous" solids obtained with quite low yields (<4 wt %) after heating at 100 °C for times shorter than 18 h gave one very broad ^{29}Si line around −95 ppm (Figure 2c). When the crystallization time was increased to 2 days, this ^{29}Si line disappeared and $Q^4(n\text{Al})$ ^{29}Si lines with n = 3−0 began to be resolved, in good agreement with the growth of UZM-9LS crystals (Figure 3). However, the ^{27}Al MAS NMR spectra of all of the solids obtained at crystallization times ranging from 3 h to 18 days, although amorphous, were characterized by only one broad line around 53 ppm (Figure S1 in the Supporting Information), typical of tetrahedral Al.[12a]

The ^{13}C chemical shift of TMA$^+$ in zeolites is particularly sensitive to the size of the cavity inside which it becomes entrapped during zeolite synthesis, although it is practically independent of the Si/Al ratio of the zeolite host.[12a] It has been repeatedly shown that the TMA$^+$ ions occluded within the *lta*-cage and the smaller *sod*-cage in LTA zeolites exhibit ^{13}C NMR chemical shifts around 57 and 59 ppm, which are shifted to lower field by ca. 1 and 3 ppm, respectively, relative to the corresponding line of TMA$^+$ in D_2O.[16] This stimulated us to investigate the entire process of nucleation and growth of UZM-9LS crystals using ^{13}C MAS NMR spectroscopy. Figure 4 shows the ^{13}C MAS NMR spectra of the solid products recovered after UZM-9LS crystallization at 100 °C for different times. The spectrum of the product recovered after 3 h of heating, which has an organic content of 7.6 wt % (Table 1), showed a strong TMA$^+$ CH_3 ^{13}C NMR line at 57.0 ppm. Elemental analysis indicated a small decrease in organic content of this amorphous solid to 6.0 wt % when the sample was refluxed twice in 1.0 M $NaNO_3$ solution for 4 h, suggesting that

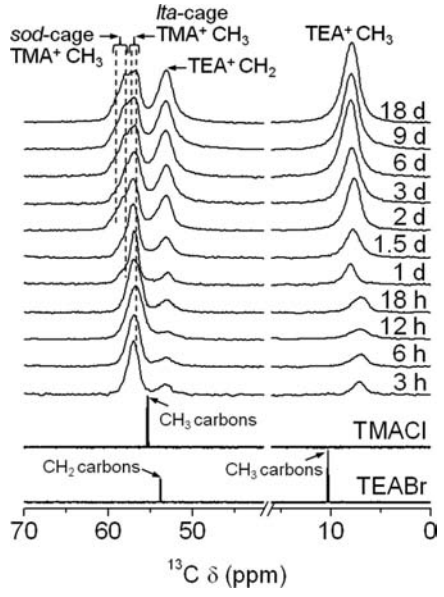

Figure 4. ^{13}C MAS NMR spectra of the solid products recovered after UZM-9LS crystallization at 100 °C for different times. To display the changes in the ^{13}C NMR line intensities more clearly, the relative intensities are referenced to the height of the ^{13}C line around 57 ppm due to CH_3 groups of TMA$^+$ ions in *lta*-cages. The ^{13}C solution NMR spectra of TMACl and TEABr in D_2O (bottom traces) are also included for comparison.

its organics (including TMA$^+$) are mainly located in nonexchangeable sites, probably in *lta*-cages and/or cages that are similar to and readily transformed into *lta*-cages.

Interestingly, a new shoulder around 58 ppm began to appear in the ^{13}C MAS NMR spectrum of the solid obtained after 1 day of heating, the relative crystallinity (ca. 20%) of which was still low (Figure 3). This shoulder, which also comes from TMA$^+$, became stronger in products heated for up to an additional 5 days, as ascertained by curve decomposition (Figure S2 in the Supporting Information and Table 2). A combination of elemental and ^{13}C MAS NMR analyses revealed the presence of ca. 0.9 TMA$^+$ ions per *sod*-cage in fully crystallized UZM-9LS obtained after 6 days of heating, in addition to ca. 0.8 TMA$^+$ ions per *lta*-cage. Because this sample

dx.doi.org/10.1021/ja309831e | J. Am. Chem. Soc. 2013, 135, 2248−2255

Table 1. Chemical Composition Data for a Series of Solid Products Recovered after Heating at 100 °C for Various Times during UZM-9LS Synthesis

time (days)	%N	%C	%H	∑CHN[a]	TEA^+/TMA^+ [b]	% TEA^+	% TMA^+	$\%Na^+$	%Si	%Al	Si/Al[c]	Na^+/Al	TMA^+/Al	TEA^+/Al	T_{max} (°C)[d]
0.125	1.02	3.84	2.74	7.61 (9.0)	0.10 (0.18)	1.14	6.47	4.77	21.1	8.17	2.48	0.69	0.29	0.03	320
0.25	1.18	4.51	2.74	8.44 (9.6)	0.11 (0.19)	1.37	7.07	4.90	22.4	8.59	2.50	0.67	0.30	0.03	330
0.5	0.77	2.97	2.37	6.12 (7.0)	0.13 (0.19)	1.14	4.98	5.51	22.5	8.50	2.54	0.76	0.21	0.03	320
0.75	1.19	5.06	2.82	9.07 (10.8)	0.30 (0.26)	3.13	5.94	5.17	23.7	8.86	2.57	0.68	0.24	0.07	330
1	1.08	4.72	2.62	8.32 (7.7)	0.36 (0.27)	3.23	5.09	5.28	23.6	8.70	2.67	0.71	0.21	0.08	340
1.5	1.43	6.51	2.81	10.76 (12.1)	0.45 (0.54)	4.75	6.01	4.60	25.3	8.55	2.84	0.63	0.25	0.11	350
2	1.49	7.12	2.97	11.58 (11.6)	0.62 (0.56)	6.04	5.54	4.31	24.8	8.30	2.87	0.61	0.24	0.15	350
3	1.68	8.37	3.25	13.29 (13.7)	0.79 (0.87)	7.73	5.56	3.52	25.1	7.73	3.12	0.53	0.26	0.21	350
6[e]	1.97	9.87	3.31	15.15 (14.7)	0.82 (0.89)	8.95	6.20	2.80	25.7	7.70	3.21 (3.2)	0.43	0.29	0.24	350
9	1.98	10.06	3.30	15.34 (15.4)	0.89 (0.97)	9.36	5.98	2.77	26.0	7.34	3.40 (3.2)	0.44	0.29	0.26	350
18	1.97	9.92	3.30	15.19 (14.8)	0.84 (0.95)	9.06	6.13	2.59	24.6	7.12	3.32 (3.2)	0.43	0.31	0.26	350

[a]Total organic content in wt %. Values in parentheses are exothermic weight losses determined by TGA/DTA at 250−800 °C. [b]Values in parentheses are TEA^+/TMA^+ ratios calculated from the relative intensities of the CH_3 and CH_2 ^{13}C NMR lines of TMA^+ and TEA^+ ions, respectively. [c]Values in parentheses are Si/Al ratios calculated from the ^{29}Si MAS NMR data. [d]Temperature of the exothermic peak maximum in DTA. [e]From a combination of elemental and thermal analyses, this sample was determined to have the unit cell composition $TEA_{10.9}TMA_{13.3}Na_{19.5}H_{1.9}(H_2O)_{80.8}[Al_{45.6}Si_{146.4}O_{384}]$. H^+ was introduced to make this zeolite electrically neutral.

Table 2. Chemical Shifts, Line Widths, and Relative Intensities of ^{13}C MAS NMR Resonances of TMA^+ and TEA^+ Ions within the Solid Products Recovered after Heating at 100 °C for Various Times during UZM-9LS Synthesis

	^{13}C NMR δ (ppm from TMS)[b]					
	TMA^+ CH_3[c]				TEA^+ CH_2	TEA^+ CH_3
sample[a]	*sod*-cage		*lta*-cage		*lta*-cage	
TMACl	55.3				–	
TEABr	–				53.8	10.4
3 h	–	–	–	57.0 (110) [1.00]	53.3 (120) [0.18]	7.2 (110) [0.25]
6 h	–	–	–	57.0 (130) [1.00]	53.2 (150) [0.19]	7.0 (140) [0.26]
12 h	–	–	–	56.8 (160) [1.00]	53.0 (170) [0.19]	7.2 (170) [0.27]
18 h	–	–	–	56.9 (140) [1.00]	53.1 (160) [0.26]	7.1 (150) [0.29]
1 day	–	58.4 (90) [0.19]	–	57.0 (90) [1.00]	53.0 (100) [0.32]	7.8 (100) [0.51]
1.5 days	–	58.4 (100) [0.23]	–	57.0 (100) [1.00]	53.2 (140) [0.67]	7.8 (140) [0.84]
2 days	59.5 (90) [0.08]	58.4 (110) [0.34]	–	57.0 (120) [1.00]	53.2 (130) [0.80]	7.7 (120) [1.03]
3 days	59.1 (80) [0.08]	57.9 (100) [0.45]	–	56.8 (120) [1.00]	53.2 (160) [1.33]	7.9 (140) [1.64]
6 days	59.3 (100) [0.16]	58.1 (110) [0.89]	57.5 (50) [0.11]	56.9 (90) [0.89]	53.3 (170) [1.83]	8.1 (130) [2.27]
9 days	59.3 (100) [0.16]	58.1 (120) [0.91]	57.5 (60) [0.11]	56.9 (110) [0.89]	53.2 (170) [2.13]	8.0 (140) [2.69]
18 days	59.2 (100) [0.21]	58.1 (100) [0.79]	57.4 (60) [0.19]	56.7 (90) [0.81]	53.2 (160) [1.91]	8.0 (130) [2.36]

[a]The first two samples are the pure reagents; the remaining samples are the solids obtained at the indicated times. [b]Values in parentheses and square brackets are full widths at half-maximum in Hz and relative intensities referenced to the intensity of the peak(s) appearing around 57 ppm due to decomposed component(s) from TMA^+ in *lta*-cages, respectively. [c]Each *lta*-cage in fully crystallized UZM-9LS zeolite obtained after 6 days of heating contained 0.8 TMA^+ ions and 1.4 TEA^+ ions, whereas there were 0.9 TMA^+ ions per *sod*-cage. Because this material also contained ca. 20 Na^+ ions per unit cell, we tentatively assigned the two TMA^+ CH_3 ^{13}C NMR lines at 57.5 and 59.3 (±0.2) ppm, detectable from highly crystalline UZM-9LS samples only, to the TMA^+ ions present together with TEA^+ and/or Na^+ in *lta*-cages and with Na^+ in *sod*-cages, respectively.

also contained ca. 20 Na^+ ions per unit cell (Table 1), we tentatively assigned the two additional TMA^+ CH_3 ^{13}C NMR lines at 57.5 and 59.3 (±0.2) ppm, detectable from highly crystalline LTA materials only, to the TMA^+ ions present together with TEA^+ and/or Na^+ in *lta*-cages and with Na^+ in *sod*-cages, respectively, which are thus in more restricted environments. Therefore, we reasoned that the formation of *lta*-cages and/or such similar cages occurs at the nucleation stage of UZM-9LS in the solid phase and/or at the solid−liquid interface and takes precedence over that of *sod*-cages.

The ^{13}C MAS NMR spectra in Figure 4 also show two lines around 53 ppm and 7 or 8 ppm due to the CH_2 and CH_3 carbons of TEA^+, respectively. These ^{13}C NMR lines became stronger as the crystallization time increased from 1 to 6 days, indicating a continuous increase in the relative concentration of TEA^+ in the solid phase. The same conclusion can be drawn from the chemical composition data for solid products obtained in this work (Table 1). It thus appears that the role of TMA^+ as both an organic SDA and an initiator of aluminosilicate condensation during UZM-9LS nucleation is greater than that of TEA^+. This was further supported by the striking enrichment of TMA^+ in all of the products relative to the starting synthesis solution (TEA^+/TMA^+ = 16), the ^{13}C solution NMR spectrum of which showed hardly any TMA^+ CH_3 ^{13}C NMR line (Figure S3 in the Supporting Information). In contrast, the opposite holds for the crystal growth process: for crystallization times longer than 18 h, the TEA^+ CH_3 ^{13}C NMR line shifted to lower field (7 to 8 ppm), indicative of a more restricted environment than seen for TEA^+ at the nucleation stage.

To gain information on the *d4r*-cage evolution during UZM-9LS crystallization at 100 °C, we compared the IR spectra of a series of solid products taken at different time intervals (Figure

dx.doi.org/10.1021/ja309831e | J. Am. Chem. Soc. 2013, 135, 2248−2255

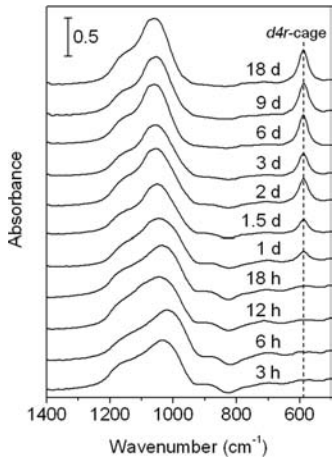

Figure 5. IR spectra in the structural region of the solid products recovered after UZM-9LS crystallization at 100 °C for different times.

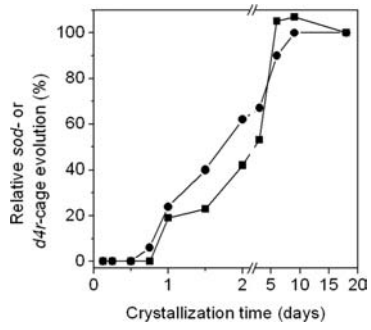

Figure 6. Relative intensities of the ^{13}C NMR line for CH_3 groups of TMA^+ ions in *sod*-cages (■) and of the *d4r*-cage IR band (●) for the solid products recovered after UZM-9LS crystallization at 100 °C for different times.

5). A weak IR band at 590 cm^{-1} due to the *d4r* unit[17] was detectable in products obtained after at least 1 day of heating. Like the ^{13}C NMR line for CH_3 groups of TMA^+ ions in *sod*-cages (Figure 6), its intensity increased until UZM-9LS fully crystallized at 6 days. Since the detection limit of IR spectroscopy with respect to the atomic ordering of zeolites is superior or similar to that of NMR spectroscopy,[18] it is clear that the nucleation process is initiated by the formation of *lta*-cages, which is followed by the construction of *sod* and *d4r*-cages at least in an almost simultaneous manner. We should note here that trends essentially identical to those described so far were also observed during the long-established synthesis of ZK-4,[19] another Si-rich LTA zeolite, in which TMA^+ and Na^+ are used as SDAs (Figure S4 in the Supporting Information).

To address further the issue discussed above, we performed quantum-chemical calculations of the stabilization energies for various combinations of Na^+, TMA^+, and/or TEA^+ ions in four different cage systems of the LTA structure: a discrete *sod*-cage, a discrete *lta*-cage, and systems containing 1 *lta*-cage + 12 *d4r*-cages or 1 *lta*-cage + 8 *sod*-cages + 12 *d4r*-cages, each with one or two Al atoms in tetrahedral positions (Figure S5 in the Supporting Information). Under the assumption that the Na^+ ion in zeolite synthesis mixtures exists as an octahedral $[Na(H_2O)_6]^+$ complex, as in aqueous solution,[8] the termination of the *lta*-cage surface with *d4r*-cages was calculated to be thermodynamically less favorable by 7−43 kcal/mol of SDA than the formation of a discrete *lta*-cage or the system containing 1 *lta*-cage + 8 *sod*-cages + 12 *d4r*-cages (i.e., a complete LTA unit cell) (Table 3). There is one high-resolution transmission electron microscopy study showing that the surface of a large single crystal of zeolite A is terminated with a layer of incomplete *sod*-cages rather than with *d4r*-cages.[20] This implies that the formation of *sod*-cages over the *lta*-cage surface is more feasible than the formation of *d4r*-cages, consistent with the results of our calculations. On the other hand, when no TMA^+ was added to our synthesis solution, we were unable to obtain any crystalline solid even after 4 weeks of heating. We also obtained the same result in the complete absence of Na^+, suggesting that both TMA^+ and Na^+ ions are indispensable for promoting UZM-9LS nucleation.

Figure 7 shows the formation pathway for high-silica LTA zeolite crystals emerging from the overall results of our work. Small (alumino)silicate species are organized around the organic SDAs (mainly TMA^+ ions) and/or the hydrated Na^+ ion to make large *lta*-cages at the nucleation stage in the solid phase, regardless of their structural incompletion. In fact, all of the amorphous solids obtained after heating at 100 °C for less

Table 3. Stabilization Energies Calculated for Various Combinations of SDAs in Four Different Cage Systems of the LTA Structure

		stabilization energy (kcal/mol of SDA)[c]			
Al/system[a]	guest cation(s)[b]	*sod*	*lta*	1 *lta* + 12 *d4r*[d]	1 *lta* + 8 *sod* + 12 *d4r*[d]
1	1 $[Na(H_2O)_6]^+$	−14.1	−117.9	−104.8	−118.7
	1 TMA^+	−50.3	−109.1	−100.0	−106.7
	1 TEA^+	103.5	−93.8	−85.6	−92.6
2	2 $[Na(H_2O)_6]^+$	−[e]	−312.1	−269.6	−292.2
	1 $[Na(H_2O)_6]^+$ + 1 TMA^+	−[e]	−257.8	−229.1	−255.2
	1 $[Na(H_2O)_6]^+$ + 1 TEA^+	−[e]	−246.3	−219.2	−237.2
	2 TMA^+	−[e]	−241.7	−213.7	−229.6
	1 TMA^+ + 1 TEA^+	−[e]	−232.6	−199.0	−220.4

[a]The number of tetrahedral Al atoms in the framework of the given cage system. [b]In general, the Na^+ ion in aqueous solution forms the octahedral aqua complex $[Na(H_2O)_6]^+$.[8] This argument led us to assume that the Na^+ ion in zeolite synthesis mixtures is present as $[Na(H_2O)_6]^+$ and not as its dehydrated form, although the structure of hydrated Na^+ ions could be altered according to the pH of the synthesis solution and the presence of the other reactant components in this crystallization. The lowest-energy structure for the octahedral $[Na(H_2O)_6]^+$ complex in which the bond distance between an O atom of a water molecule and the Na^+ ion was fixed at 2.37 Å[8] was derived using the ONIOM method.[9] [c]The SDA includes both organic (TEA^+ and TMA^+) and inorganic (Na^+) cations. [d]The guest species are assumed to be located within the *lta*-cage only. [e]Not calculated because the *sod*-cage cannot accommodate more than one of either TMA^+, TEA^+, or $[Na(H_2O)_6]^+$ without severe steric hindrance.

dx.doi.org/10.1021/ja309831e | J. Am. Chem. Soc. 2013, 135, 2248−2255

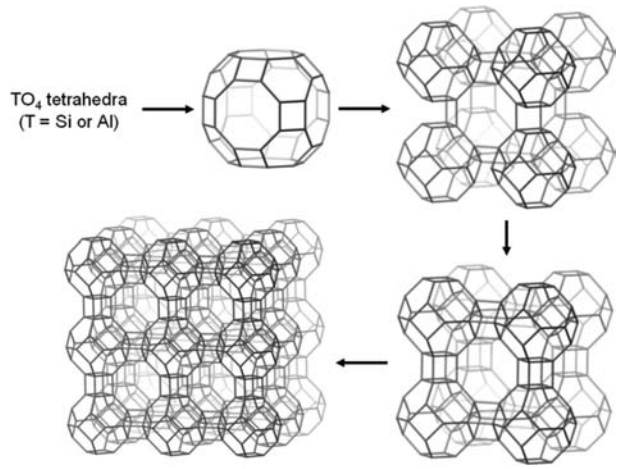

Figure 7. Schematic illustration of the high-silica LTA zeolite formation pathway in the $TEA^+/TMA^+/Na^+$ mixed-SDA system.

than 18 h gave $(TMA^+ + Na^+)/Al$ ratios very close to unity, supporting the role of these ions as the initiators of aluminosilicate condensation during UZM-9LS nucleation (Figure 8). These solids also have low Si/Al ratios (2.5)

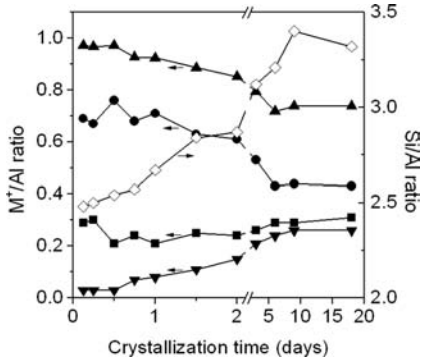

Figure 8. TMA^+/Al (■), Na^+/Al (●), $(TMA^+ + Na^+)/Al$ (▲), TEA^+/Al (▼), and Si/Al (◇) ratios in the solid products recovered after UZM-9LS crystallization at 100 °C for different times.

compared with that of the synthesis mixture (8), since highly charged aluminosilicates are the most insoluble in the presence of Na^+ and TMA^+. Once such a single *lta*-cage is formed, the cations balancing the negative framework charges created by Al substitution can be placed not only inside this large cage but also in the proximity of its outer surface. The very high TMA^+ occupancy of *sod*-cages in fully crystallized UZM-9LS (0.9) supports the conclusion that TMA^+ ions as well as Na^+ ions residing outside the preorganized large cage may promote the continuous consumption of relatively simple aluminosilicate species (mainly *d3r* units) in the solution phase (Figure 2b), resulting in the construction of smaller *sod*-cages around the *lta*-cage. In view of the calculation results described above, a logical next step would be coupling among the *sod*-cages (i.e., *d4r*-cage formation), leading to embryonic LTA crystals. Finally, a similar self-assembly process in which TEA^+ is also involved may allow LTA nuclei to substantially grow at higher Si/Al ratios (Figure 8).

Our work also sheds light on the course of events in the CDM method for zeolite synthesis. After the initial condensation by Na^+ and TMA^+, the growth step embodies the process for which the CDM approach[7] was designed (i.e., to foster the cooperation of TEA^+, TMA^+, and Na^+), as these ions are incorporated from the aluminosilicate solution into the LTA zeolite crystals with a higher Si/Al ratio. Indeed, during this period from 18 h to 6 days, the TEA^+/Al ratio of the solid products increased from 0.07 to 0.24. Also, their TMA^+/Al ratio increased slightly from 0.24 to 0.29. However, while the Na^+/Al ratio decreased from 0.63 to 0.43, the Si/Al ratio increased from 2.57 to 3.21 (Table 1 and Figure 8). Furthermore, as shown in Figure 3, UZM-9LS crystallization was characterized by a low yield (ca. 20 wt %) even after 18 days of heating at 100 °C. This implies that the majority of the synthesis mixture remained in solution during the synthesis. The predilection of solid products for incorporating TMA^+ and especially Na^+ may in our view explain why their concentrations must be kept low in order to maintain the aluminosilicate solutions that allow the cooperation of all three SDAs during the UZM-9LS crystal growth process. Finally, it is interesting to note that this same synthesis mixture, when heated at 150 °C, yielded UZM-5 with a higher Si/Al ratio (ca. 7) in much higher yield (ca. 45 wt %).[7b] A mechanistic study of the synthesis of this particular zeolite is currently underway in our laboratory.

■ CONCLUSIONS

Our work provides the first example in which the pathway for formation of zeolites from their discrete building units has been clearly elucidated. The construction of large *lta*-cages was found to precede that of much smaller *sod* or *d4r*-cages at the nucleation stage of high-silica LTA zeolite in the $TEA^+/TMA^+/Na^+$ mixed-SDA system. In this CDM synthesis, both Na^+ and TMA^+ play an important role in the initial condensation and nucleation, while the crystal growth takes place in an aluminosilicate solution with the incorporation of Na^+, TMA^+, and TEA^+ into the solid phase. We also believe that the combination of ex-situ ^{13}C MAS NMR and IR techniques employed here, although far from state-of-the-art, will be quite useful for obtaining invaluable information on the molecular-level mechanisms responsible for the synthesis of other industrially important zeolites such as FAU and CHA materials in the presence of both organic and inorganic SDAs.

■ ASSOCIATED CONTENT

Supporting Information

Complete ref 11; solution and solid-state ^{27}Al and ^{13}C NMR spectra of a series of mother liquors and solid products recovered after UZM-9LS crystallization at 100 °C for different times; Powder XRD patterns and ^{13}C MAS NMR and IR spectra of the solid products recovered after ZK-4 crystallization at 80 °C for different times; and the four different cage systems with one and two framework Al atoms of the LTA structure employed in the quantum-chemical calculations of the stabilization energies for various combinations of TMA^+, TEA^+, and hydrated Na^+ ions. This material is available free of charge via the Internet at http://pubs.acs.org.

■ AUTHOR INFORMATION

Corresponding Author

sbhong@postech.ac.kr

Notes

The authors declare no competing financial interest.

■ ACKNOWLEDGMENTS

This work was supported by UOP LLC and the National Creative Research Initiative Program (2012R1A3A2048833) through the National Research Foundation of Korea. We thank Prof. K. Seff (University of Hawaii) for helpful discussions.

■ REFERENCES

(1) (a) Davis, M. E.; Zones, S. I. In *Synthesis of Porous Materials*; Occelli, M. L., Kessler, H., Eds.; Marcel Dekker: New York, 1997; pp 1−34. (b) Davis, M. E. *Nature* **2002**, *417*, 813−821. (c) Camblor, M. A.; Hong, S. B. In *Porous Materials*; Bruce, D. W., O'Hare, D., Walton, R. I., Eds.; Wiley: Chichester, U.K., 2011; pp 265−325.

(2) Cundy, C. S.; Cox, P. A. *Microporous Mesoporous Mater.* **2005**, *82*, 1−78.

(3) Barrer, R. M.; Baynham, J. W.; Bultitude, F. W.; Meier, W. M. *J. Chem. Soc.* **1959**, 195−208.

(4) (a) Epping, J. D.; Chmelka, B. F. *Curr. Opin. Colloid Interface Sci.* **2006**, *11*, 81−117. (b) Knight, C. T. G.; Wang, J.; Kinrade, S. D. *Phys. Chem. Chem. Phys.* **2006**, *8*, 3099−3103. (c) Knight, C. T. G.; Balec, R. J.; Kinrade, S. D. *Angew. Chem., Int. Ed.* **2007**, *46*, 8148−8152. (d) Follens, L. R. A.; Aerts, A.; Haouas, M.; Caremans, T. P.; Loppinet, B.; Goderis, B.; Vermant, J.; Taulelle, F.; Martens, J. A.; Kirschhock, C. E. A. *Phys. Chem. Chem. Phys.* **2008**, *10*, 5574−5583.

(5) (a) Shi, J.; Anderson, M. W. *Chem. Mater.* **1996**, *8*, 369−375. (b) Mintova, S.; Olson, N. H.; Valtchev, V.; Bein, T. *Science* **1999**, *283*, 958−960. (c) Valtchev, V. P.; Bozhilov, K. N. *J. Am. Chem. Soc.* **2005**, *127*, 16171−16177. (d) Aerts, A.; Kirschhock, C. E. A.; Martens, J. A. *Chem. Soc. Rev.* **2010**, *39*, 4626−4642. (e) Ren, L.; Li, C.; Fan, F.; Guo, Q.; Liang, D.; Feng, Z.; Li, C.; Li, S.; Xiao, F.-S. *Chem.—Eur. J.* **2011**, *17*, 6162−6169.

(6) Baerlocher, Ch.; McCusker, L. B. Database of Zeolite Structures. http://www.iza-structure.org/databases/.

(7) (a) Moscoso, J. G.; Lewis, G. J.; Gisselquist, J. L.; Miller, M. A.; Rohde, L. M. U.S. Patent 6,713,041, 2004. (b) Lewis, G. J.; Miller, M. A.; Moscoso, J. G.; Wilson, B. A.; Knight, L. M.; Wilson, S. T. *Stud. Surf. Sci. Catal.* **2004**, *154*, 364−372. (c) Kim, S. H.; Park, M. B.; Min, H.-K.; Hong, S. B. *Microporous Mesoporous Mater.* **2009**, *123*, 160−168.

(8) Richens, D. T. *The Chemistry of Aqua Ions*; Wiley: Chichester, U.K., 1997.

(9) Boronat, M.; Martínez-Sánchez, C.; Law, D.; Corma, A. *J. Am. Chem. Soc.* **2008**, *130*, 16316−16323.

(10) (a) Zhao, Y.; Truhlar, D. *Theor. Chem. Acc.* **2008**, *120*, 215−241. (b) Hohenstein, E. G.; Chill, S. T.; Sherrill, C. D. *J. Chem. Theory Comput.* **2008**, *4*, 1996−2000.

(11) Frisch, M. J.; et al. *Gaussian 09*, revision A.02; Gaussian, Inc.: Wallingford, CT, 2009.

(12) (a) Engelhardt, G.; Michel, D. *High-Resolution Solid-State NMR of Silicates and Zeolites*; Wiley: Chichester, U.K., 1987. (b) Thangaraj, A.; Kumar, R. *Zeolites* **1990**, *10*, 117−120. (c) Cheng, C.-H.; Shantz, D. F. *J. Phys. Chem. B* **2006**, *110*, 313−318.

(13) Jacobs, P. A.; Derouane, E. G.; Weitkamp, J. *J. Chem. Soc., Chem. Commun.* **1981**, 591−593.

(14) Caratzoulas, S.; Vlachos, D. G. *J. Phys. Chem. B* **2008**, *112*, 7−10.

(15) Harris, R. K.; Samadi-Maybodi, A.; Smith, W. *Zeolites* **1997**, *19*, 147−155.

(16) (a) Jarman, R. H.; Melchior, M. T. *J. Chem. Soc., Chem. Commun.* **1984**, 414−416. (b) Hayashi, S.; Suzuki, K.; Shin, S.; Hayamizu, K.; Yamamoto, O. *Chem. Phys. Lett.* **1985**, *113*, 368−371. (c) Mihailova, B.; Mintova, S.; Karaghiosoff, K.; Metzger, T.; Bein, T. *J. Phys. Chem. B* **2005**, *109*, 17060−17065.

(17) Flanigen, E. M.; Khatami, H.; Szymanski, H. A. *Adv. Chem. Ser.* **1971**, *101*, 201−229.

(18) Burkett, S. L.; Davis, M. E. *Chem. Mater.* **1995**, *7*, 920−928.

(19) Kerr, G. T. *Inorg. Chem.* **1966**, *5*, 1537−1539.

(20) Wakihara, T.; Sasaki, Y.; Kato, H.; Ikuhara, Y.; Okubo, T. *Phys. Chem. Chem. Phys.* **2005**, *7*, 3416−3418.